BB

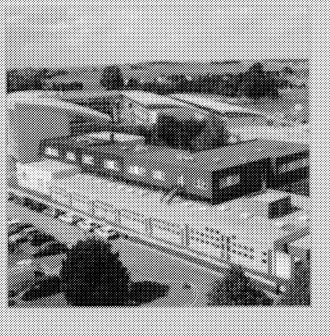

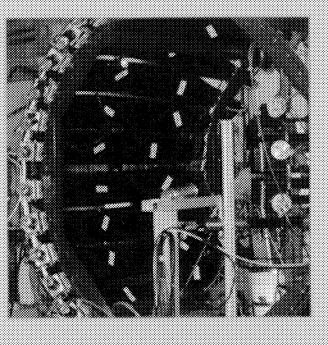

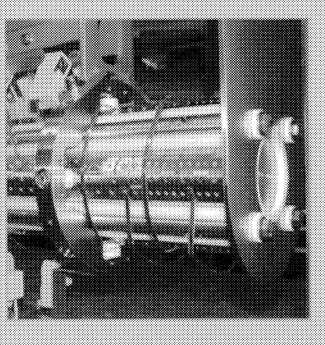

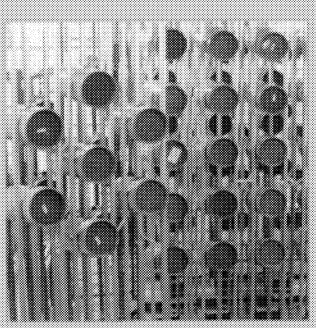

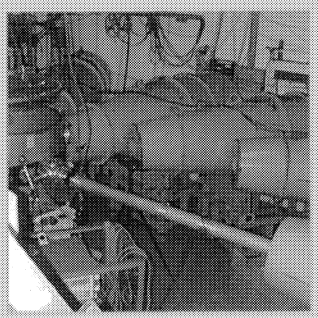

UNIVERSITÉ DE CAEN / BASSE-NORMANDIE

U.F.R. DE SCIENCES

ÉCOLE DOCTORALE : SIMEM

(Structure, Information, Matière Et Matériaux)

LABORATOIRE DE PHYSIQUE CORPUSCULAIRE

INSTITUT DES SCIENCES DE LA MATIÈRE ET DU RAYONNEMENT

Bimodality in binary Au + Au collisions from 60 to 100 MeV/u.

M. Pichon, B. Tamain, R. Bougault, F. Gulminelli, O. Lopez, M.L. Begemann-Blaich, R. Bittiger, B. Borderie, A. Chbihi, P. Chomaz, R. Dayras, D. Durand, C. Escano-Rodriguez, J.D. Frankland, E. Galichet, D. Gourio, D. Guinet, B. Guiot, S. Hudan, P. Lautesse, F. Lavaud, A. Le Fevre, N. Le Neindre, J. Lukasik, U. Lynen, A. Mignon, W.F.J. Muller, L. Manduci, J. Marie, L. Nalpas, H. Orth, M. Parlog, M.F. Rivet, E. Rosato, A. Saija, C. Schwarz, C. Sfienti, W. Trautmann, A. Trzcinski, K. Turzo, A. Van Lauwe, E. Vient, M. Vigilante, C. Volant, J.P. Wieleczko, B. Zwieglinski.

(INDRA and ALADIN collaborations)

March 2003 **LPCC 03-04**

Contribution to the XLI International Winter Meeting on Nuclear Physics, Bormio, 2003

Bimodality in binary Au + Au collisions from 60 to 100 MeV/u

M. Pichon[1], B. Tamain[1], R. Bougault[1], F. Gulminelli[1], O. Lopez[1], M.L. Begemann-Blaich[2], R. Bittiger[2], B. Borderie[3], A. Chbihi[4], P. Chomaz[4], R. Dayras[5], D. Durand[1], C. Escano-Rodriguez[4], J.D. Frankland[4], E. Galichet[3,7], D. Gourio[2], D. Guinet[8], B. Guiot[4], S. Hudan[4], P. Lautesse[8], F. Lavaud[3], A. Le Fèvre[2], N. Le Neindre[3], J. Lukasik[2,10], U. Lynen[2], A. Mignon[4], W.F.J. Müller[2], L. Manduci[1], J. Marie[4], L. Nalpas[5], H. Orth[2], M. Pârlog[9], M.F. Rivet[3], E. Rosato[6], A. Saija[2], C. Schwarz[2], C. Sfienti[2], W. Trautmann[2], A. Trzcinski[11],K. Turzo[2], A. Van Lauwe[1], E. Vient[1], M. Vigilante[6], C. Volant[5], J.P. Wieleczko[4], B. Zwieglinski[11]

(INDRA and ALADIN collaborations)

[1] *LPC, IN2P3-CNRS, ENSICAEN et Université, F-14050 Caen Cedex, France.*
[2] *Gesellshaft für Schwerionenforschung mbH, D-64291 Darmstadt, Germany.*
[3] *Institut de Physique Nucléaire, IN2P3-CNRS, F-91406 Orsay Cedex, France.*
[4] *GANIL, CEA et IN2P3-CNRS, B.P. 5027, F-14076 Caen Cedex, France.*
[5] *DAPNIA/SPhN, CEA/Saclay, F-91191 Gif sur Yvette, France.*
[6] *Dipartemento di Scienze Fiziche e Sezione INFN, Università di Napoli « Federico II », I-80126 Napoli, Italy.*
[7] *Conservatoire National des arts et Métiers, F-75141 Paris Cedex 03, France.*
[8] *Institut de Physique Nucléaire, IN2P3-CNRS et Université, F-69622 Villeurbanne, France.*
[9] *National Institute for Physics and Nuclear Engineering, RO-76900 Bucharest-Magurele, Romania.*
[10] *Institute of Nuclear Physics, Pl-31342 Krakov, Poland.*
[11] *A. Soltan Institute for Nuclear Studies, Pl-00681 Warsaw,Poland.*

Contribution to the XLI International Winter Meeting on Nuclear Physics, Bormio, 2003

Bimodality in binary Au + Au collisions from 60 to 100 MeV/u

M. Pichon[1], B. Tamain[1], R. Bougault[1], F. Gulminelli[1], O. Lopez[1], M.L. Begemann-Blaich[2], R. Bittiger[2], B. Borderie[3], A. Chbihi[4], P. Chomaz[4], R. Dayras[5], D. Durand[1], C. Escano-Rodriguez[4], J.D. Frankland[4], E. Galichet[3,7], D. Gourio[2], D. Guinet[8], B. Guiot[4], S. Hudan[4], P. Lautesse[8], F. Lavaud[3], A. Le Fèvre[2], N. Le Neindre[3], J. Lukasik[2,10], U. Lynen[2], A. Mignon[4], W.F.J. Müller[2], L. Manduci[1], J. Marie[4], L. Nalpas[5], H. Orth[2], M. Pârlog[9], M.F. Rivet[3], E. Rosato[6], A. Saija[2], C. Schwarz[2], C. Sfienti[2], W. Trautmann[2], A. Trzcinski[11],K. Turzo[2], A. Van Lauwe[1], E. Vient[1], M. Vigilante[6], C. Volant[5], J.P. Wieleczko[4], B. Zwieglinski[11]

(INDRA and ALADIN collaborations)

[1] *LPC, IN2P3-CNRS, ENSICAEN et Université, F-14050 Caen Cedex, France.*
[2] *Gesellshaft für Schwerionenforschung mbH, D-64291 Darmstadt, Germany.*
[3] *Institut de Physique Nucléaire, IN2P3-CNRS, F-91406 Orsay Cedex, France.*
[4] *GANIL, CEA et IN2P3-CNRS, B.P. 5027, F-14076 Caen Cedex, France.*
[5] *DAPNIA/SPhN, CEA/Saclay, F-91191 Gif sur Yvette, France.*
[6] *Dipartemento di Scienze Fiziche e Sezione INFN, Università di Napoli « Federico II », I-80126 Napoli, Italy.*
[7] *Conservatoire National des arts et Métiers, F-75141 Paris Cedex 03, France.*
[8] *Institut de Physique Nucléaire, IN2P3-CNRS et Université, F-69622 Villeurbanne, France.*
[9] *National Institute for Physics and Nuclear Engineering, RO-76900 Bucharest-Magurele, Romania.*
[10] *Institute of Nuclear Physics, Pl-31342 Krakov, Poland.*
[11] *A. Soltan Institute for Nuclear Studies, Pl-00681 Warsaw,Poland.*

Abstract: The deexcitation of quasi-projectiles (QP) released in binary Au on Au collisions has been studied from 60 to 100 MeV/u. Bimodality between two different decay patterns has been observed for intermediate violence collisions. The main experimental result is that the system jumps from one mode to the other on a narrow range of energy deposit and/or impact parameter. The sorting of the events (according to the violence of the collision) has been provided by the perpendicular energy of the light charged particles emitted on the quasi-target side. Such a sorting prevents spurious autocorrelation effects between the sorting variable and the observed mechanism. The two modes of the QP decay correspond on the one side to residue or fission fragments production, and on the other side to the multifragmentation channel. A detailed study has been performed in order to try to establish the origin of the observed bimodality in disentangling dynamical or geometrical effects from bulk matter properties linked with a liquid-gas type phase transition. The whole set of data is coherent with a dominant role of the deposited excitation energy as it is expected from theoretical arguments (lattice gas model) in the framework of a liquid-gas phase transition picture.

I- Introduction.

Multifragmentation is a process which takes place in intermediate energy heavy ion collisions and it is presently attempted to link the opening of this decay channel and the underlying liquid-gas phase transition which is expected in this energy range. Several signatures of this link have been proposed in the literature. First the fact that multifragmentation exhibits a threshold around 3MeV/u deposited excitation energy[1]. Negative heat capacities observed for several systems have also been interpreted as a possible signature of phase transition of an isolated system[2,3]. Correlations between the sizes of the outgoing fragments have also been carefully investigated: delta scaling[4], Fisher scaling[5], increased probability for a decay involving equal size fragments[6], bimodality[7], i.e. the possibility for the system of jumping at a given temperature from a condensed state (liquid) to a diluted one (gas).

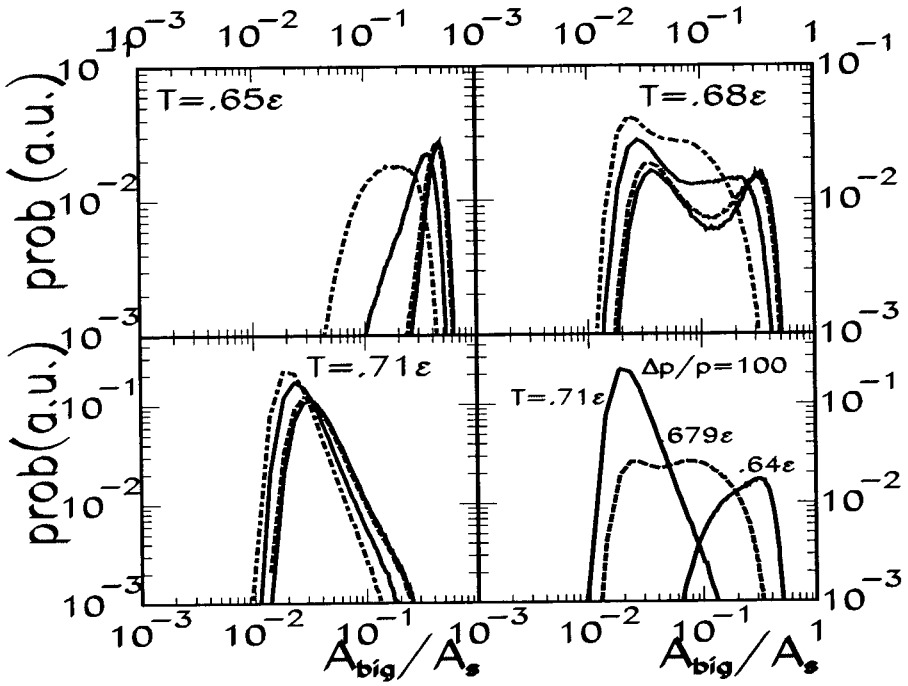

Figure 1: Canonical lattice-gas calculations for a system of 216 interacting particles. ε is their mutual interacting energy. The plots are A_{big} / A_s distributions in log-log scales ; A_{big} is the mass of the heaviest fragment emitted from a source of size A_s. The 3 first plots correspond to temperatures respectively below, at and above the liquid-gas transition temperature. The solid line distributions correspond to fully equilibrated systems. For the other curves an additional directed linear momentum Δp has been introduced: it represents 10% (dashed), 50% (dotted), 100% (dotted-dashed) of the total thermalized momentum p. The last plots (lower-right corner) correspond to various temperatures for a proportion of directed energy per particle equal to the equilibrated one (Δp/p = 100%).

In this paper we will concentrate on this bimodality signal. The reason for this choice is explained in the present section. It is connected with a fundamental difficulty: a phase transition is a process rather well defined only for an equilibrated system. But multifragmentation is observed in collisions, i.e. in processes, which, of course, exhibit many out-of-equilibrium features. Is it possible to observe a phase transition behavior in such processes? Theoretical arguments indicate that bimodality could be a robust signal in the sense that it is not strongly affected if a sizeable fraction of the available energy has not been shared among all the available degrees of freedom. Figure 1 illustrates this statement. It has been obtained in a lattice-gas calculation for an ensemble of 216 interacting particles. To deal with the fact that the system is open, no sharp boundary condition has been applied and the freeze-out volume has been treated as an observable fixed only on average in the framework of the information theory[8]. The calculation has been performed in the canonical ensemble at three temperatures slightly below the transition temperature (upper-left corner), at the transition temperature (upper-right corner), and above its value (lower-left corner). The plots indicate the probabilities of observing a given mass A_{big} for the heaviest released fragment. A_{big} has been normalized to the source size A_s. Various curves correspond to various approaches of equilibrium: the solid one has been calculated in assuming full equilibrium; for the others, an extra linear momentum has been added in a given direction (let say: the beam direction). Its proportion is resp. 10, 50, 100% of the thermalized one for resp. dashed, dotted and dashed-dotted curves. The calculation results indicate that, in the equilibrium case (solid lines), the (A_{big} / A_s) probability curve is peaked at large (resp. low) values below (resp. above) the transition temperature, whereas it exhibits a double-hump behavior at the transition temperature. The observation of a bimodal distribution for the A_{big} observable univocally characterizes the phenomenon as a first order phase transition and defines A_{big} as the order parameter of the transition[9]. This result is not dramatically modified when the additional aligned linear momentum is introduced even if its contribution reaches 50% of the thermalized one. This means that the bimodality signal is still observed if an additional dynamical (aligned) linear momentum (reflecting the entrance channel memory) is included in the calculation.

Such a result is not true for all observables. For instance, it has been established in lattice-gas calculations that the negative heat capacity signal is rapidly blurred if a dynamical energy contribution is introduced[8].

II- The studied system and the data analysis.

Following the conclusions of the discussion of the previous section, the results presented in this paper are dealing with bimodality in multifragmentation studies. We concentrated on peripheral and semi peripheral Au + Au collisions from 60 to 100 MeV/u. These systems have been studied with Indra at GSI (Indra –Aladin collaborations). At all energies, one has used the fact that collisions are mainly binary, justifying the reconstruction of a quasi-projectile (QP) and a quasi-target (QT). This statement is illustrated in figures 2 and 3. Figure 2 is a center of mass (cm) velocity diagram for alpha particles. Various plots correspond to various centralities (as explained below). For the first six bins, the binary character of the collisions is clearly evidenced (see the Coulomb rings corresponding to the QP and QT respectively). In figure 3 a similar behavior is obtained from the charge-cm velocity plots along the beam axis for all the Intermediate Mass Fragments (IMF: Z=3) which are forward emitted (in the cm frame). Most of them (and especially the two biggest ones) can be unambiguously attributed to the QP since the velocity distributions exhibit a minimum at

mid-rapidity. This statement is quite clear at 100MeV/u and slightly questionable at 60 MeV/u.

In each case, the QP has been reconstructed by putting together the forward-emitted products (IMF and Light Charged Particles – LCP-) in the cm frame. The bimodality behavior has been looked for in its decay. All the events have been retained provided the total reconstructed QP charge exceeds 65. This condition was imposed in order to ensure that no drawback due to a fragment loss could affect the results.

Let us consider now the event sorting. It has been performed from the transverse energy E_{t12} of LCP on the QT side. Since the decay analysis is made for the QP, this sorting ensures a decorrelation (no experimental drawback) between the sorting itself and the QP observables. Moreover, if equilibrium is achieved, one is closer to a canonical description where the QT plays the role of a (small) heat bath. The corresponding temperature (linked with E_{t12}) may be considered as fixed for the QP. If it is close to the liquid-gas transition temperature, one may expect to observe a bimodality in the QP distributions.

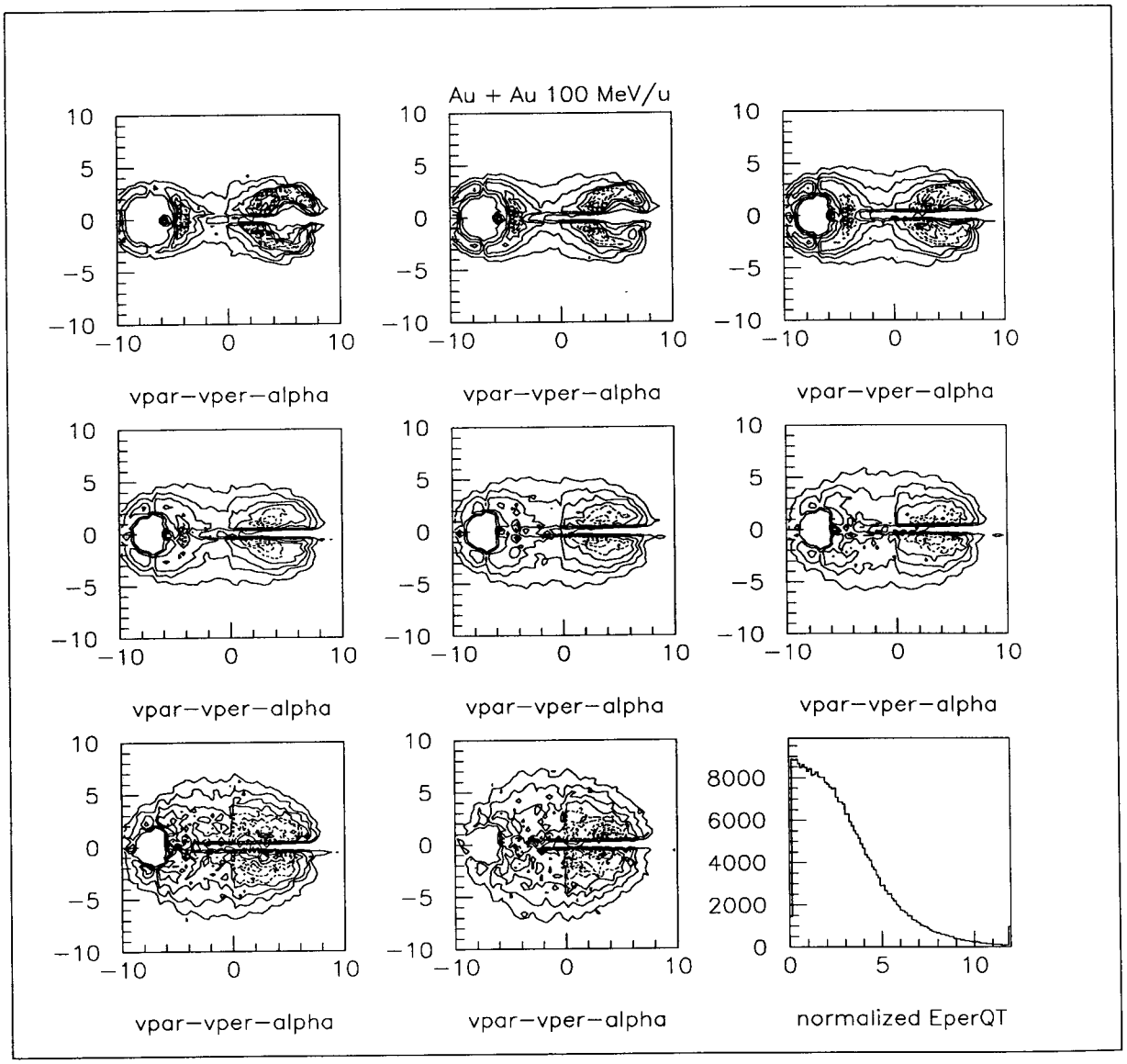

Figure 2: Alpha particle velocity diagrams (v_{par}- v_{per} plots in c unit) in the center of mass frame for various collision centralities. The last diagram is the E_{t12}^{N} distribution used to sort the events (see text). In most v_{par} - v_{per} plots the binary character of the collision is clearly evidenced.

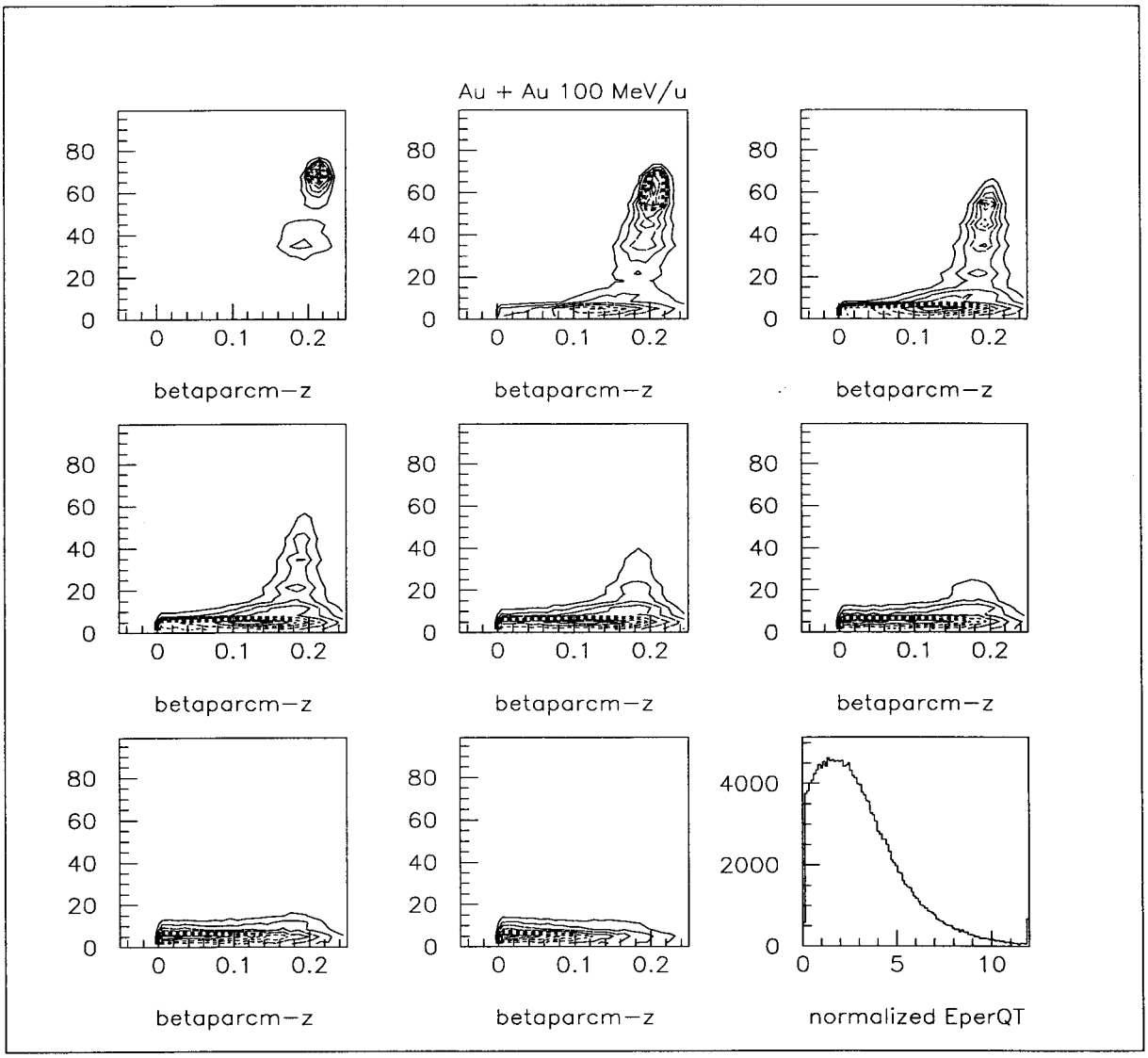

Figure 3: Correlations between the cm velocity along the beam axis (in c unit) and the charge number for all the IMF (Z≥3) emitted in the forward direction in the cm frame. Eight plots correspond to various impact parameter selections from peripheral to central collisions. The last diagram is the E_{t12}^{N} distribution used to sort the events plotted in the other diagrams. It is different from the corresponding distribution of figure 2 for very peripheral events because events with only one IMF have been rejected.

The E_{t12} distributions are shown in figure 4. E_{t12} has been normalized to the incident energy ($E_{t12}^{N} = E_{t12} / E_{inc}$). E_{t12} is expressed in MeV and E_{inc} in MeV/u. With this definition, it turns out that the range of the normalized sorting variable E_{t12}^{N} is about the same for the three considered incident energies (60, 80 and 100 MeV/u). The whole E_{t12}^{N} range has been divided into 8 equal bins, which are used now to study the bimodality signal.

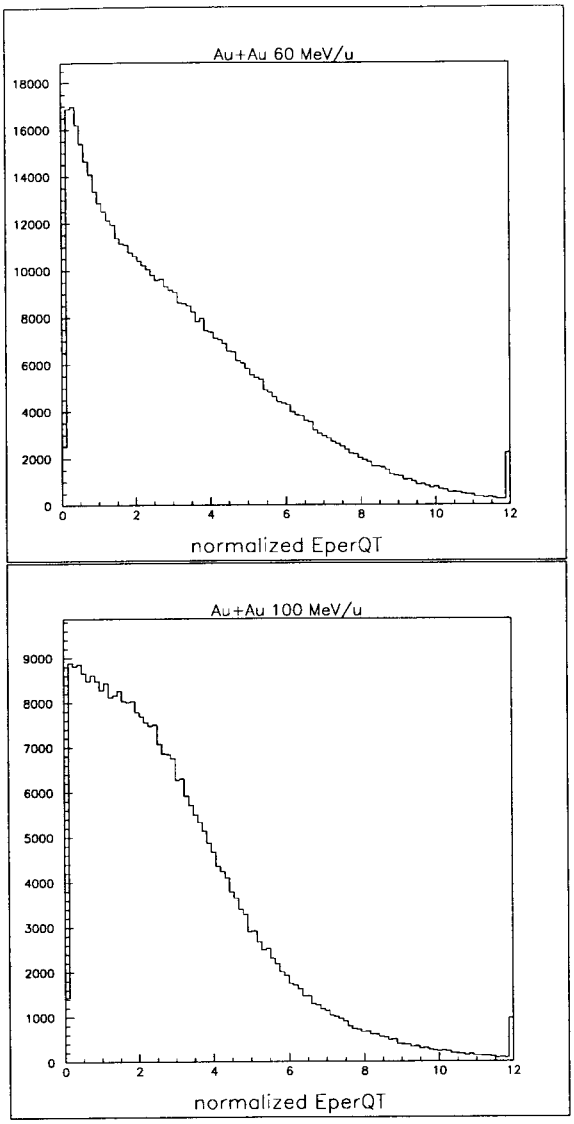

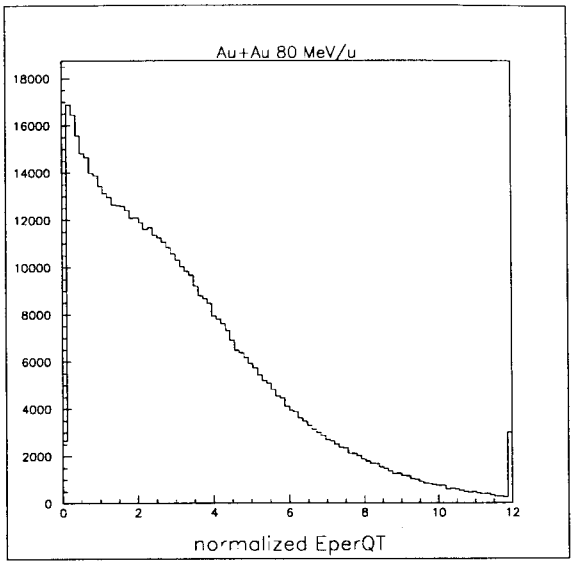

Figure 4: Total transverse energy distributions for LCP on the QT side. Transverse energy values expressed in MeV have been normalized to the incident energy (expressed in MeV/u). For the 3 studied bombarding energies, the range of the normalized transverse energy E_{t12}^{N} is about the same. It has been divided in 8 equal bins used to study the bimodality behavior of the QP in figures 5-7.

III- The bimodality observable.

We have now to make a guess concerning the possible order parameter of the transition. Remind that any observable such that the event cloud splits into two different distributions separated by a minimum can play the role of an order parameter. In particular, Ising model calculations[10] suggest that A_{big} can be an order parameter; however it is the case only if the system is in contact with a thermal bath. Any extra constraint connected to an even loose energy conservation can suppress the bimodality in A_{big} because of the obvious correlation between A_{big} and the deposited energy. However any other observable correlated to A_{big} (and less strongly correlated with the energy) may still be bimodal at the transition temperature. In this work we have chosen the asymmetry between the two heaviest fragments:

$$x_{sym} = (Z_{max} - Z_{max-1}) / (Z_{max} + Z_{max-1}).$$

In the case of fission events (which could be easily identified), we defined Z_{max} as the sum of the two fission fragment charges in order to consider on the same footing the two mechanisms referring to normal density nuclear matter (residue production and fission). Fission was selected by the fact that the charges of the two heaviest detected QP fragments exceed 25

charge units. With this definition of x_{sym} one gets the results of figure 5 where the twodimensional plots x_{sym}-Z_{max} are shown for the eight bins of E_{t12}^{N} in the case of the 100 MeV/u bombarding energy. Most of the events are localized in the up-right corner (x_{sym} and Z_{max} large) for the first three bins whereas we have the reverse situation for bins 5 to 8. These two extreme situations may be regarded as a dominance of two different modes which could be linked with liquid and gas phases. In the fourth bin, both edges of the distribution are filled with a hollow between the two maxima. Bimodality is observed for this bin in which one may say that the system can exist in both modes as it is expected for a phase transition.

Quite similar results have been obtained at the two other bombarding energies. For instance, figure 6 refers to the 60 MeV/u case.

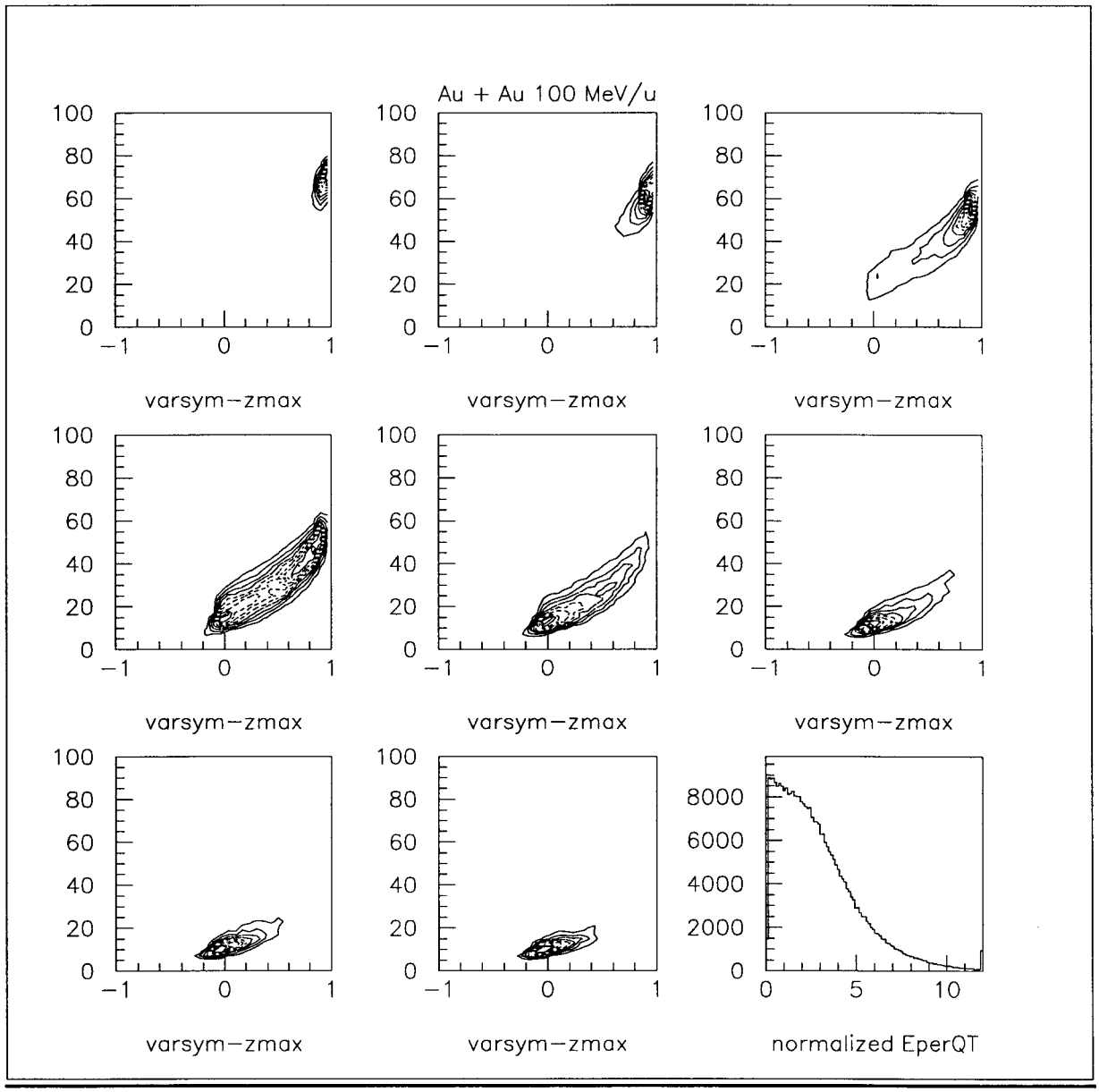

Figure 5: x_{sym}-Z_{max} plots for the 8 centrality bins selected from the E_{t12}^{N} distributions (last plot). The bimodality is observed for the fourth bin. Au + Au system at 100 MeV/u.

One may worry about the fact that fission events had a peculiar treatment in the previous figures. To get rid of this problem, another asymmetry variable x'_{sym} has been defined for which all the events have been treated in a similar way. x'_{sym} is defined as:

$$x'_{sym} = [(Z_{max} + Z_{max-1}) - (\Sigma Z_{other\ IMF})] / \Sigma Z_{all\ IMF}$$

The second term of the numerator is the total charge of the QP IMFs but the heaviest (Z_{max}) and the second heaviest (Z_{max-1}). The denominator is the total charge of the QP IMFs. x'_{sym} is not very different from x_{sym} for events for which a residue is detected since only Z_{max} is large in this case. x'_{sym} is close to x_{sym} for fission events. For multifragmentation events, the first term is about twice larger than the equivalent term of the x_{sym} formula and, because of that, the transition from one mode (possibly phase) to the other is not so well set off. Nevertheless, the main features of figures 5 and 6 are still obtained as it may be seen in figure 7 which shows the correlation between x'_{sym} and $(Z_{max} + Z_{max-1})$ for the 100 MeV/u incident energy. Similar conclusions are obtained at 80 and 60 MeV/u.

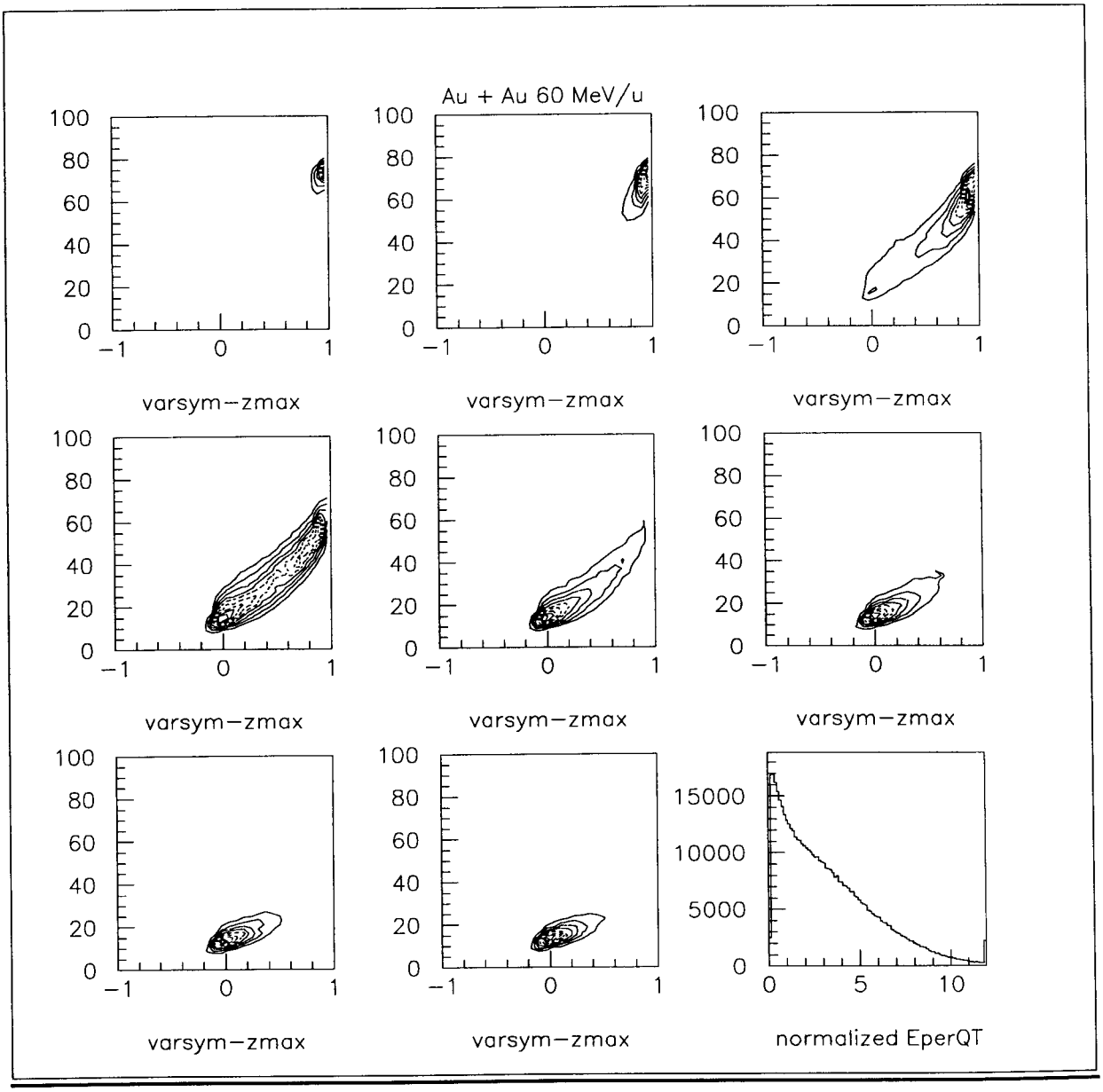

Figure 6 : Similar to figure 5 but at 60 MeV/u.

At this point, one may conclude that one observes a sudden jump from a situation for which most of the mass of the system is concentrated in one (two if fission occurs) piece, to another situation for which the available mass is shared among many pieces. The fact that this jump is sudden may be connected with a phase transition behavior between a dense phase (liquid-like) and a dilute one (gas-like).

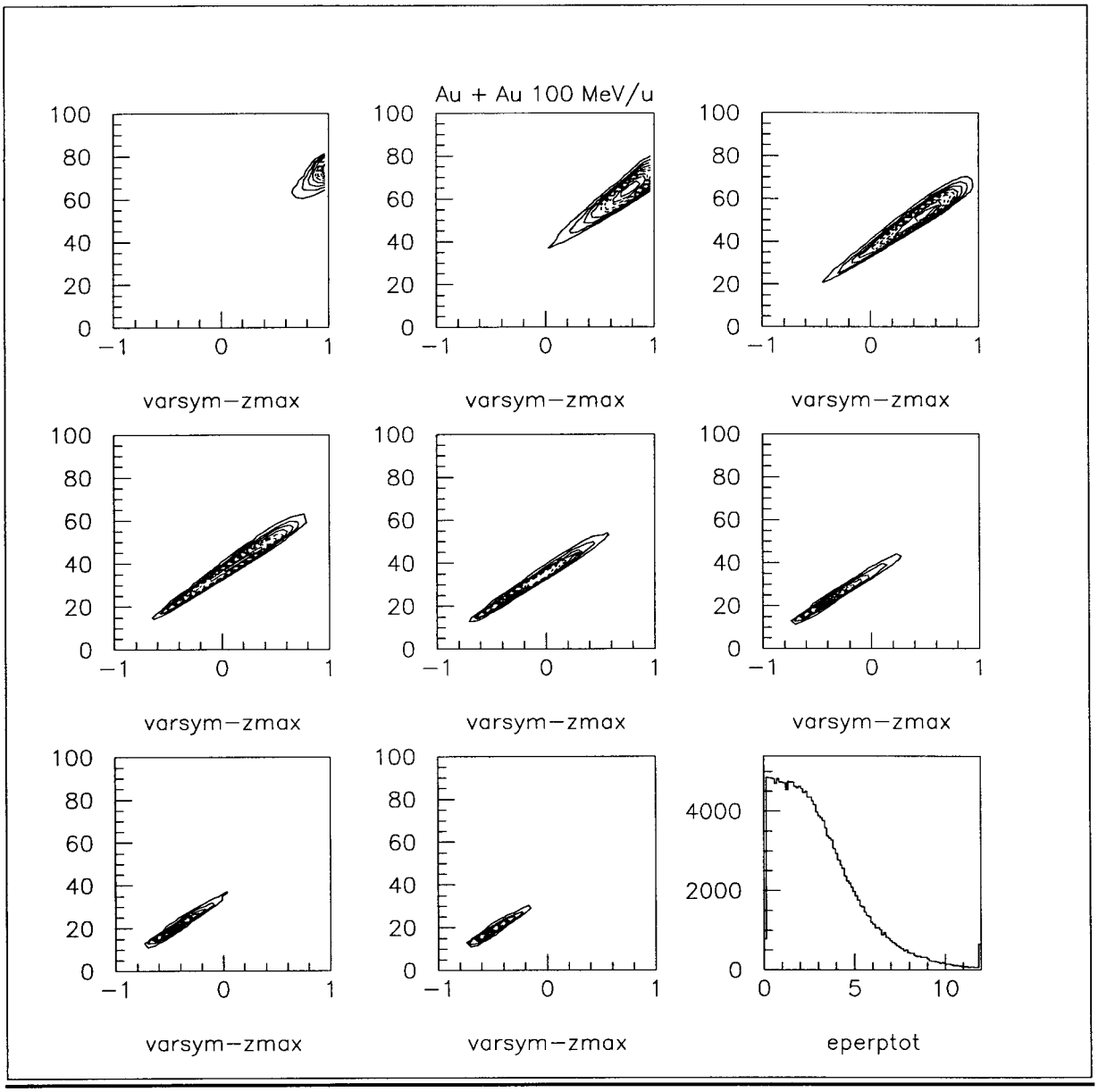

Figure 7: Similar to figure 5 but for the new asymmetry variable x'_{sym} defined in the text.

Now, the fact that this "jump" arises in the fourth bin whatever the bombarding energy is, may be interpreted in two ways. Either it signs a geometrical effect (the jump would correspond to a given impact parameter range), or it reflects the growing contribution of dynamical effects (reminiscent of the entrance channel) when the bombarding energy is increased. In this second interpretation, E_{t12} reflects both the equilibrated part of the energy and the contribution of fast processes such as nucleon-nucleon collisions. If a phase transition takes place for a given bulk energy E_{th} , the value of E_{t12} needed to reach this threshold will

increase with the incident energy because of the increasing contribution of the preequilibrium in E_{t12}.

In order to test the influence of dynamics on the results, the next section is devoted to a study of the various kinds of event topology observed at a given bombarding energy.

IV- Attempts to evidence the role of dynamics.

Let us consider the topology of the QP decay in a velocity diagram (figure 8). The angle θ is defined as the emission angle of the heaviest QP fragment relatively to its recoil direction in the center of mass frame. If the heaviest fragment was isotropically emitted from the QP, the *cos (θ)* distribution would be flat. One sees in figure 9 that it is not the case whatever the centrality of the collision is. Instead, one observes that the heaviest fragment is generally forward emitted in the QP frame. This phenomenon which has been extensively studied in reference 11 is a clear dynamical effect: the heaviest QP fragment direction is reminiscent of the initial projectile direction. We have considered two classes of events: those for which the entrance channel memory is clear (*cos (θ)* > 0.4), and those for which this memory is lost (backward emission: *cos (θ)* < -0.4). We will label "more dynamical" and "less dynamical" the events belonging respectively to these two classes.

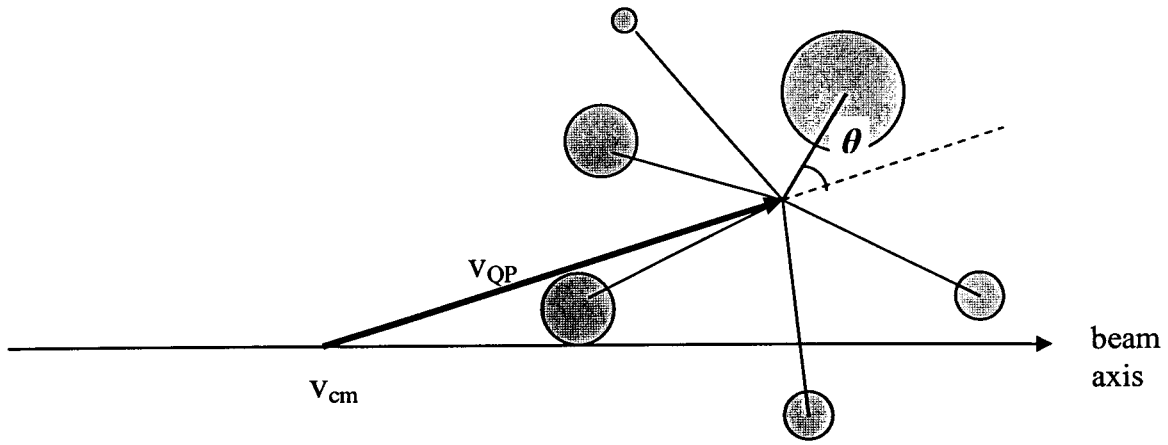

Figure 8: Velocity diagram showing a typical topology of a QP breaking. The angle θ is the emission direction of the heaviest QP decay product relatively to the QP velocity vector in the center of mass frame.

If one looks at the bimodality signals for these two classes of events, one finds the results of fig, 10 and 11, which refer respectively to "more" and "less" dynamical events. The main features of these figures are the shifts of the value of E_{t12}^{N} corresponding to bimodality. The sorting variable at the transition has larger (resp. lower) values than the one observed in figure 5 depending on the selection of "more" (resp. "less") dynamical events. It is the behavior which is expected if the relevant parameter which governs bimodality is the bulk energy stored in the QP.

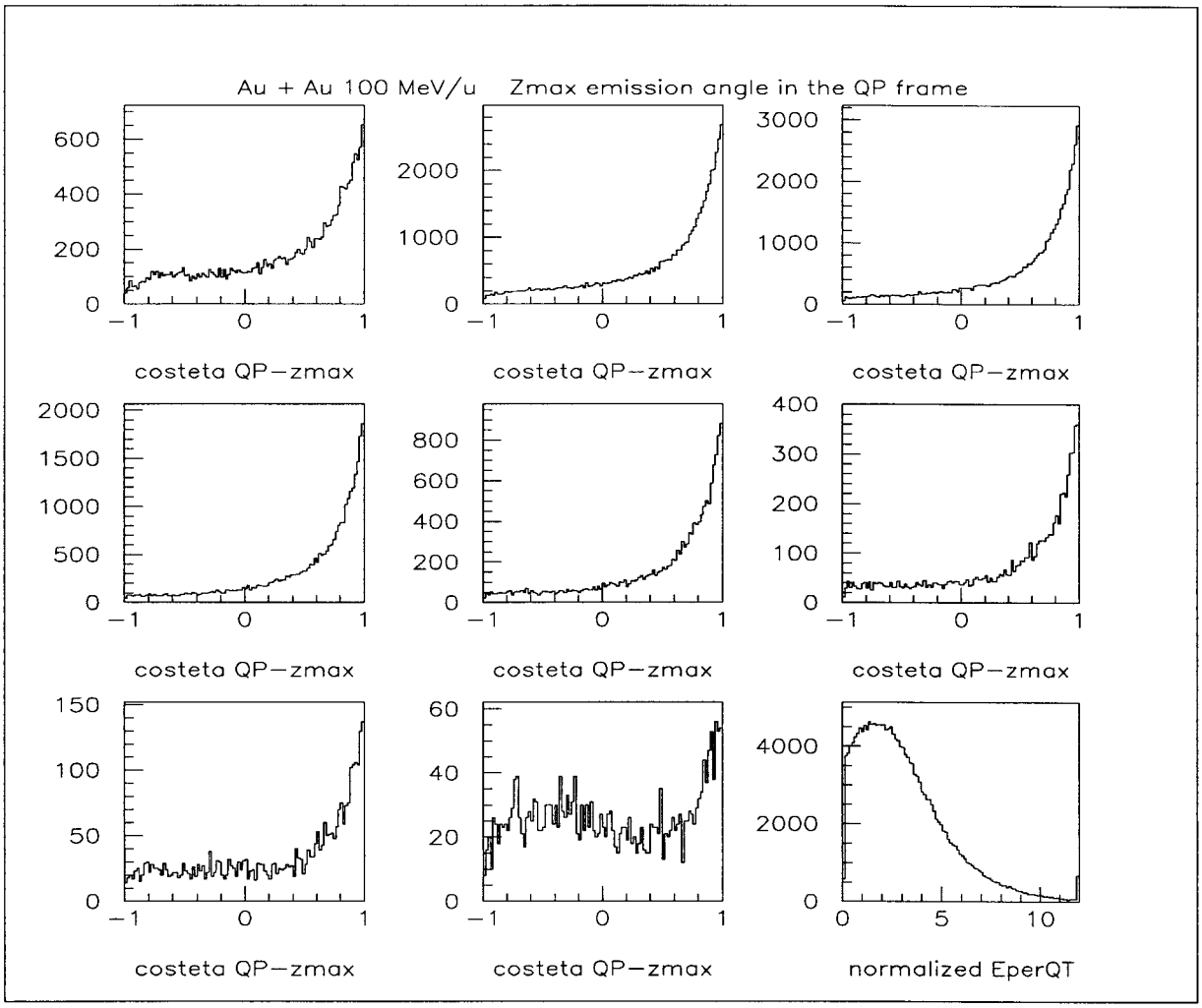

Figure 9: Angular distributions of the heaviest QP decay products. The abscissa is the cosinus of the θ angle defined in figure 8. Various plots correspond to the 8 centrality bins obtained from the E_{t12}^{N} distribution shown in the last plot. Au + Au system at 100 MeV/u.

			ΣE_{cin}^{IMF} (MeV units)					
Inc. Energy	**cos (θ)**	**dynamics**	**bin 2**	**bin 3**	**bin 4**	**bin 5**	**bin 6**	**bin 7**
100 MeV/u	> 0.4	more	2636	2122	**1778**	**1527**	1336	1192
	< -0.4	less	2518	**1964**	**1575**	1289	1060	963
80 MeV/u	> 0.4	more	2281	1845	**1545**	**1329**	1166	1041
	< -0.4	less	2282	**1741**	**1325**	1067	920	840
60 MeV/u	> 0.4	more	1809	1462	**1239**	**1077**	969	892
	< -0.4	less	1653	**1261**	**983**	835	766	716

Table 1: For each bombarding energy and for two ranges of the cos (θ) variable (see text), one has calculated the mean value (MeV units) of the sum of the center of mass kinetic energies of all the IMF attributed to the QP. This quantity ΣE_{cin}^{IMF} is connected with the kinetic energy loss in the entrance channel and to the corresponding deposited energy. The thick numbers correspond to the bins located around the jump from one mode to the other (see figure 10 and 11 for the 100 MeV/u bombarding energy). The values obtained for ΣE_{cin}^{IMF} are similar for "more" and "less" dynamical events.

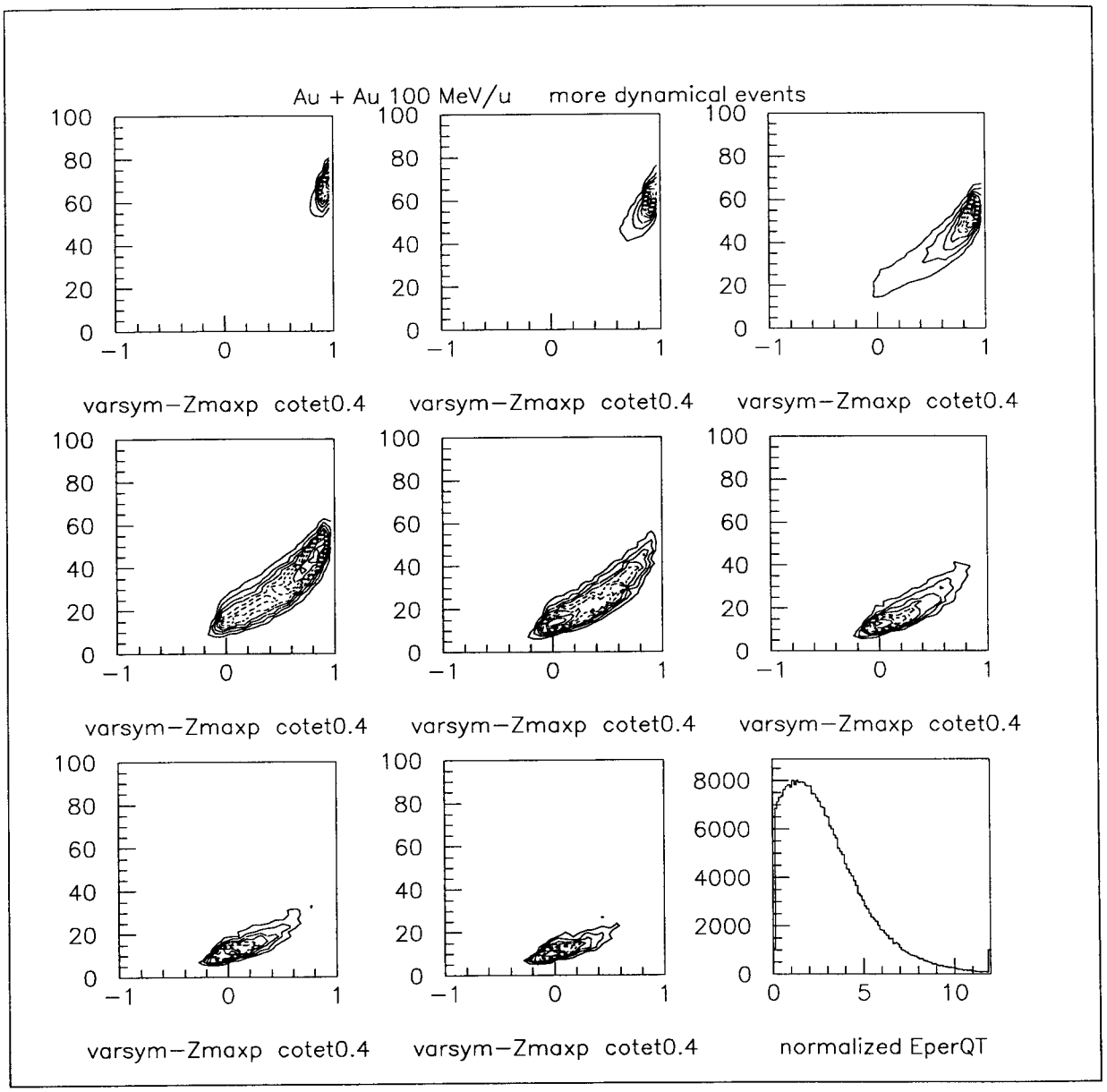

Figure 10: Similar to figure 5 but for "more dynamical" events (cos(θ) > 0.4; see text).

To be a little more quantitative, let us try to estimate the dynamical part of the available energy, i.e. the kinetic energy that is still aligned with the beam axis when the QP decay occurs. This energy (E_{dyn}) may be approximated by the sum ΣE_{cin}^{IMF} of the kinetic energy of the IMF (Z≥3) released from the QP (the E_{cin}^{IMF} values are defined in the center of mass of the reaction). This energy has been presented in table 1 for various E_{t12}^{N} bins. Values written in bold correspond to the bimodality region as it is seen at 100 MeV/u in figure 10 and 11. It turns out that, for a given bombarding energy, ΣE_{cin}^{IMF} has similar values in the bimodality region for "more" (*cos (θ)* resp. larger than 0.4) and "less" (*cos (θ)* smaller than –0.4) dynamical events. This behavior is expected if bimodality is observed only if a threshold value is reached for the bulk energy that is dissipated in the QP (i.e. if the transition is related to temperature).

V- Bimodality and the negative heat capacity signal.

A possible signature of the liquid-gas phase transition of nuclear matter has been proposed in the literature[2,3]: it is the negative heat capacity, which is expected to be observed for finite size, isolated systems. This signal has been looked for in the case of the QP decay in Au+Au collisions we are studying in this contribution.

Let us remind that the negative heat capacity may be evidenced from the fluctuations of the sharing of the available energy in the breaking source (at freeze-out) between two energy modes: for instance, the total kinetic energy of the outgoing products (E_{kin}) and the corresponding potential energy (E_{pot}). More precisely, the heat capacity may be expressed as[12]:

$$C = C_{kin}^2 / (C_{kin} - \sigma_{kin}^2/T^2) \qquad (1)$$

In this expression, C_{kin} is the partial kinetic energy heat capacity (dE_{kin}/dT) and σ_{kin}^2 is the corresponding variance (which reflects the fluctuations in the sharing of the total available energy). T is the micro-canonical temperature of the system at freeze-out. One sees from relation (1) that the total heat capacity becomes negative if the second term of the denominator exceeds the first one.

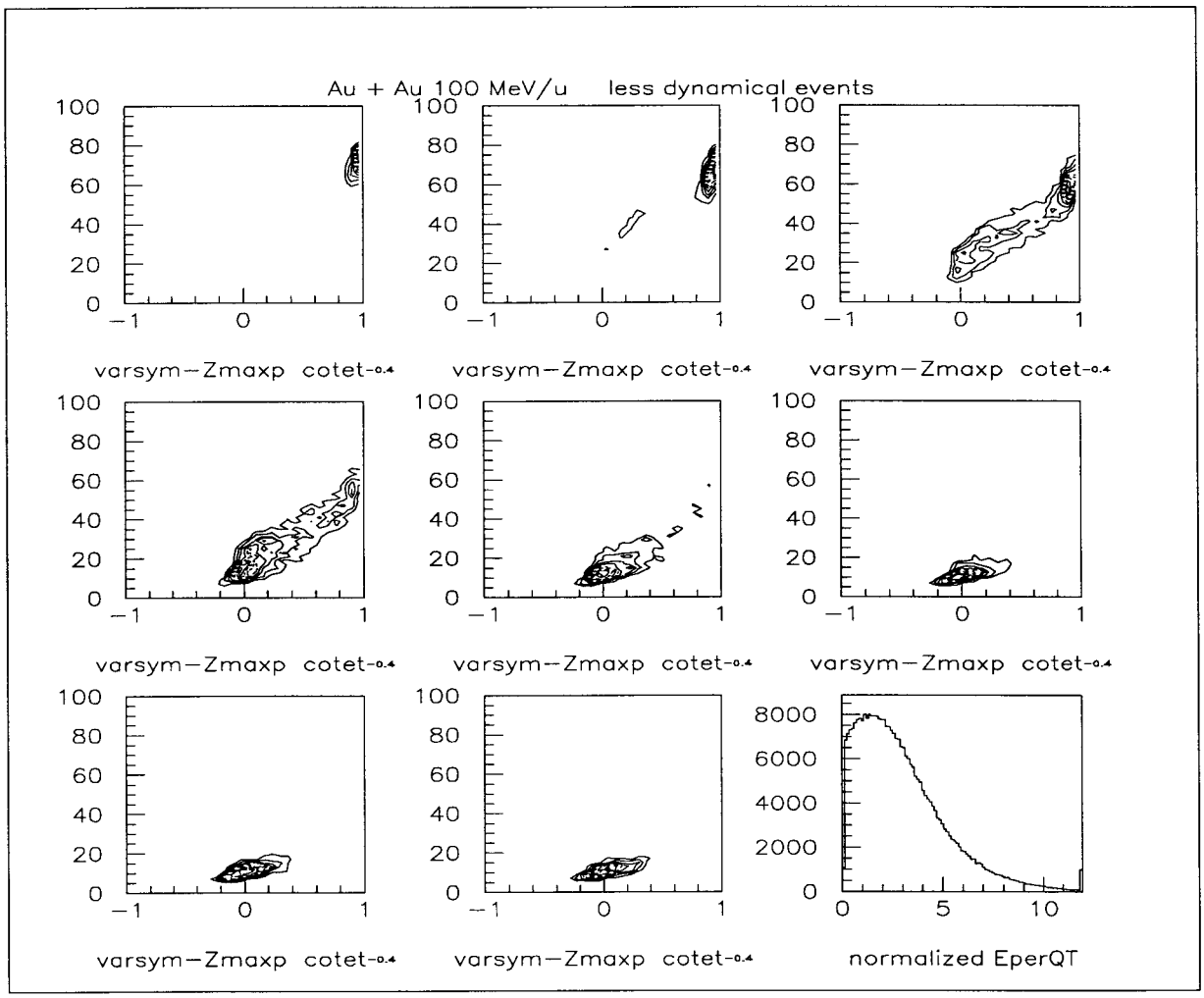

Figure 11: Similar to figure 5 and 10 but for "less dynamical" events (cos(θ) < -0.4; see text). The bimodality behavior is obtained for a smaller value, as it is expected if the bulk energy deposited in the system is the relevant parameter.

It is possible to extract all these quantities from a QP calorimetry. The method, which has been used, is described in reference 2). The excitation energy has been calculated by taking into account all the IMF attributed to the QP and the forward emitted LCP in the QP frame. This second contribution has been doubled . Neutron contribution has been included on average for each excitation energy bin. Their mean number has been obtained from the difference between the initial QP mass and the total detected mass (IMF + LCP). The mass of each IMF is deduced from its charge number by using the Epax formula[13].

The negative heat capacity signal is easily cancelled by dynamical effects. Hence, one has to select events that minimize such effects. This selection has been performed by retaining only compact events for which the relative momentum between the heaviest fragment and the center of mass of the others is smaller than a threshold. This selection ensures the cancellation of elongated events which have kept a strong memory of the beam direction. Fission events have also been removed because in this case, kinetic energy fluctuations are dominated by the fission process itself. (Fission has been recognized from the product of the charges of the two corresponding fission fragments – larger than 900 for fission events.)

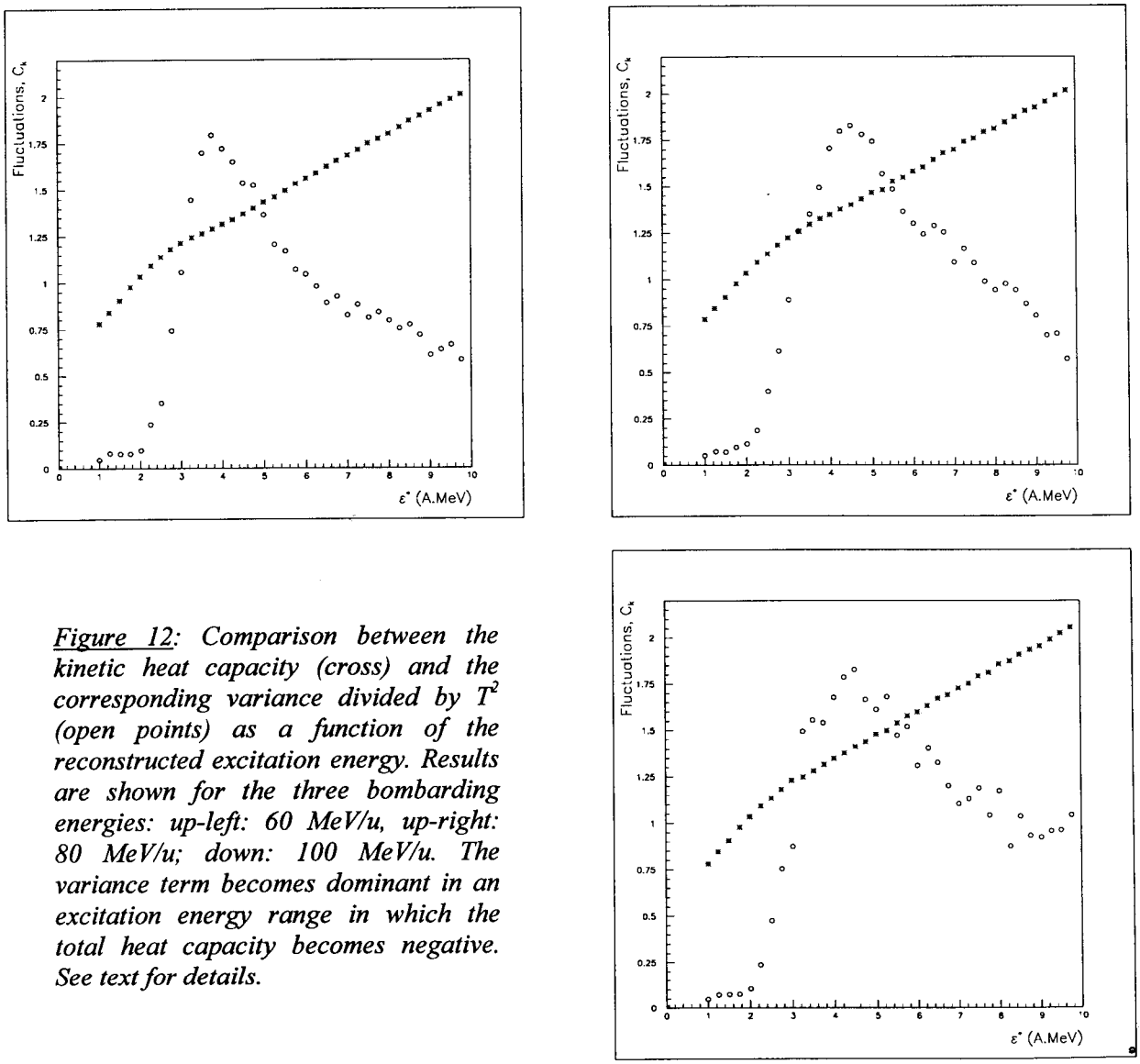

Figure 12: Comparison between the kinetic heat capacity (cross) and the corresponding variance divided by T^2 (open points) as a function of the reconstructed excitation energy. Results are shown for the three bombarding energies: up-left: 60 MeV/u, up-right: 80 MeV/u; down: 100 MeV/u. The variance term becomes dominant in an excitation energy range in which the total heat capacity becomes negative. See text for details.

With the above selection the negative heat capacity signal is clearly obtained as it is shown in figure 12 where the two terms of the denominator of relation (1) are plotted as a function of the primary QP excitation energy. For the three bombarding energies, the signal is observed in a range of about 3-5 MeV/u excitation energy.

Now, the events selected in figure 12 have been considered from the bimodality point of view. The results are shown in figure 13. For each event (fission excluded as in figure 12), one has looked at the correlation between the two heaviest fragments. The abscissa is the transverse energy E_{t12} of LCP on the QT side used to sort the bimodality events in the first part of this paper. However, note that in figure 13, this quantity has not been normalized to the beam energy as it was the case in figures 5-10. The quantity plotted on the second axis is a linear combination between Z_{max} (charge of the heaviest QP fragment) and $(Z_{max}- Z_{max-1})$ the difference between the charges of the 2 heaviest products. A large value corresponds to events with a residue; a small one is obtained for multifragment emission. At low E_{t12} values one observes a dominance of the residue production. At variance, multifragmentation is dominant for large E_{t12}. In between, bimodality is observed, but now, the transition range is the same (between 150 and 200 MeV) whatever the incident energy is. This means that, when selecting events for which dynamical effects are as low as possible, bimodality is observed for the same range of deposited energy.

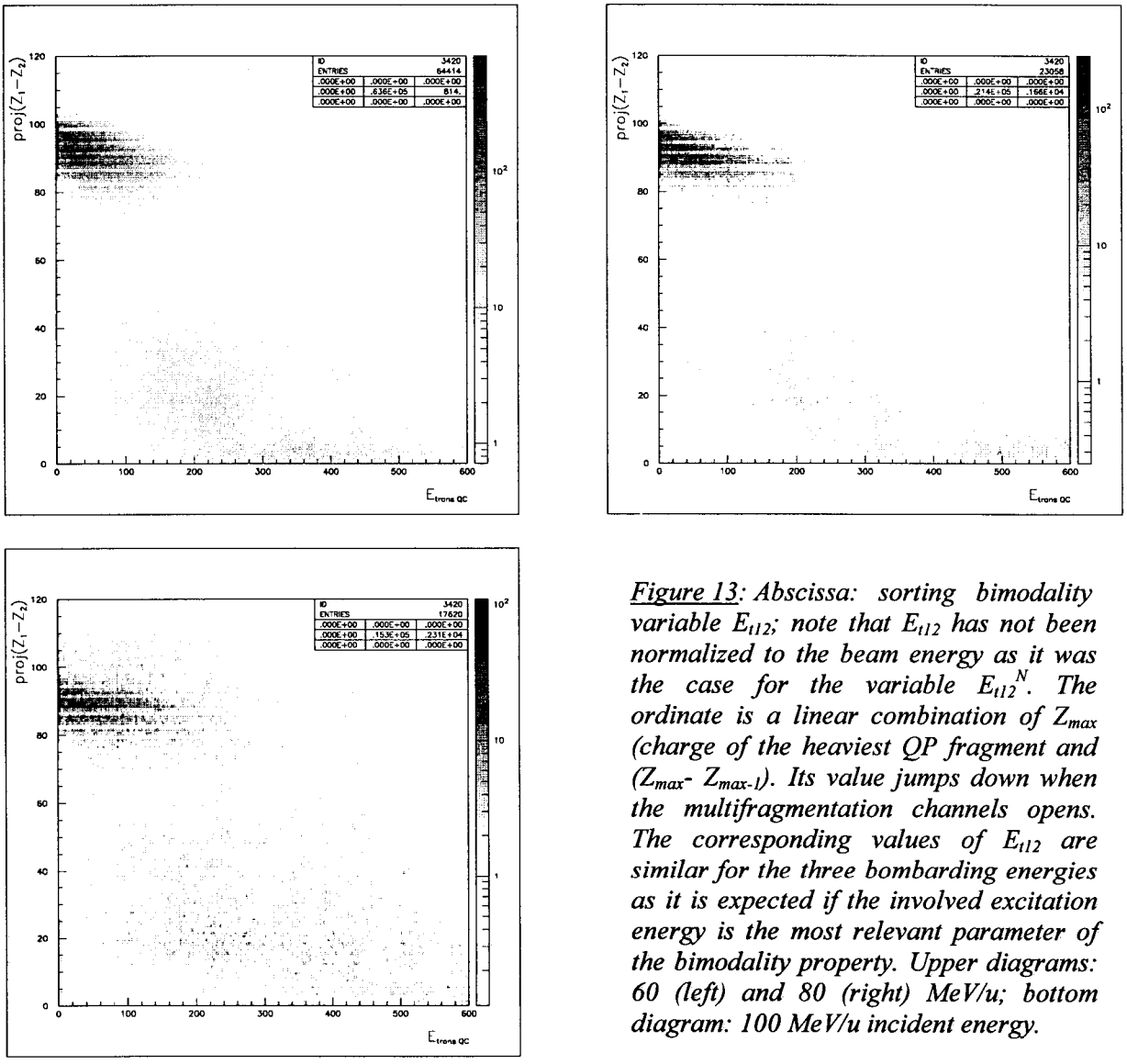

Figure 13: Abscissa: sorting bimodality variable E_{t12}; note that E_{t12} has not been normalized to the beam energy as it was the case for the variable E_{t12}^{N}. The ordinate is a linear combination of Z_{max} (charge of the heaviest QP fragment and $(Z_{max}- Z_{max-1})$. Its value jumps down when the multifragmentation channels opens. The corresponding values of E_{t12} are similar for the three bombarding energies as it is expected if the involved excitation energy is the most relevant parameter of the bimodality property. Upper diagrams: 60 (left) and 80 (right) MeV/u; bottom diagram: 100 MeV/u incident energy.

VI- Conclusion.

In this paper, we have shown that a bimodality behavior is observed in the decay of the quasi-projectiles released in peripheral and semi-peripheral Au + Au collisions from 60 to 100 MeV/u. Such observations are coherent with previous ones obtained both from Indra and Aladin data[7,14]. When sorting the events according to the total LCP transverse energy on the QT side E_{t12}, it turns out that the transition is sudden and happens for a E_{t12} value roughly proportional to the incident energy. This result that can be understood as a geometrical effect can also reflect the growing contribution of non-equilibrated energy when the incident energy is increased. This second interpretation has been analysed by looking at the topology of the events. For all incident energies the results are compatible with the following statement: bimodality is observed when a threshold has been reached for the energy which has been shared among most of the available degrees of freedom.

This statement is also supported by the negative heat capacity behavior that is observed only if compact events are selected. These events are those for which a large part of the available energy has been shared among all the degrees of freedom. By selecting these events it turns out that bimodality is observed for the same transverse energy (E_{t12}) range whatever the bombarding energy is.

All these features are compatible with a scenario in which multifragmentation is a process used by a nucleus to evolve from the liquid (dense) phase of nuclear matter to its gas (dilute) form.

References:

1- D. Durand, E. Suraud and B. Tamain, Nuclear dynamics in the nucleonic regime, IOP publishing Ltd 2001

2- M. D'Agostino et al., Nucl. Phys.A650 (1999) 329, and Proceeedings of the XXXVIII International Winter Meeting on Nuclear Physics, Bormio, 2000, p.386

3- N. Le Neindre et al., Proceeedings of the XXXVIII International Winter Meeting on Nuclear Physics, Bormio, 2000, p.404

4- R. Botet and M. Ploszajczak, Phys. Rev. E62 (2000) 1825

5- J.B. Elliott et al., Phys. Rev. Lett. 88 (2002) 042701 and ArXiv: nucl-ex/0205004

6- G. Tabacaru et al., submitted to Eur. Phys. J. A., and B. Borderie et al., Phys. Rev. Lett. 86 (2001) 3252

7- N. Bellaize et al., Nucl. Phys. A709 (2002) 367

8- F. Gulminelli and Ph. Chomaz, ArXiv: nucl-th/0209032

9- Ph. Chomaz, F. Gulminelli and V. Duflot, Phys. Rev. E64 (2001) 046114

10- F. Gulminelli et al., ArXiv: cond-mat/0302177

11- J. Colin et al., submitted to Phys. Rev C.

12- P. Chomaz and F. Gulminelli, Nuc. Phys. A647 (1999) 153

13- K. Sümmerer et al., Phys. Rev. C42 (1990) 2546, and Phys. Rev. C61 (2000) 034607

14- W.D. Kunze, PhD thesis, Universität Frankfurt (1996)